Theoret. chim. Acta (Berl.) 25, 62—82 (1972)

Porphyrins XXV. Extended Hückel Calculations on Location and Spectral Effects of Free Base Protons*

A. M. SCHAFFER** and M. GOUTERMAN

Department of Chemistry, University of Washington, Seattle, Washington 98105

Received June 14, 1971

Extended Hückel calculations for the free bases of porphin, phthalocyanine, tetrabenzporphin, and tetrazaporphin show: (i) A marked effect of carbon-nitrogen skeletal distortions is expected on the $Q_x - Q_y$ (i.e. visible) band splitting that may account for observed environment effects; (ii) bridged structures will show very little splitting without either incipient bond formation between central hydrogen and bridge nitrogen or considerable skeletal distortion; (iii) while solution phthalocyanine may be bridged, the vapor is not; (iv) $n - \pi^*$ transitions introduced by the bridge aza nitrogens may be the cause of Soret band broadening of phthalocyanine and tetrazaporphin. Band polarizations with respect to the skeleton are discussed.

Rechnungen mit der erweiterten Hückeltheorie für die freien Basen von Porphin, Phthalocyanin, Tetrabenzporphin und Tetrazaporphin zeigen, 1. daß eine Verzerrung des C–N-Gerüstes einen deutlichen Effekt auf die Aufspaltung des $Q_x - Q_y$-Bandes zeitigen sollte, 2. daß verbrückte Strukturen kaum eine Aufspaltung hervorbringen sollten wenn nicht beginnende Bindungsbildung zwischen den zentralen Wasserstoff- und den Brücken-Stickstoffatomen oder beträchtliche Verzerrungen des Gerüstes vorliegen, 3. daß Phthalocyanin vielleicht in flüssigem Zustand verbrückt ist, dagegen im gasförmigen nicht und 4. daß $n\pi^*$-Übergänge, die von den Brücken-Azastickstoffatomen induziert werden, die Ursache der Soret-Bandenverbreiterung von Phthalocyanin und Tetrazaporphin sein können. Schließlich werden Bandpolarisierungen bezüglich des C–N-Gerüstes diskutiert.

Des calculs de Hückel Etendu pour les bases libres de la porphine, de la phtalocyanine, de la tétrabenzoporphine et de la tétraazaporphine montrent que:

1) un effet marqué des distorsions du squelette carbone-azote est à attendre sur la séparation de la bande $Q_x - Q_y$ (c'est-à-dire visible), ce qui peut rendre compte des effets d'environnement observés.

2) les structures pontées présenteront peu de séparation s'il n'y a pas soit formation d'un début de liaison entre l'hydrogène central et l'azote du pont soit une distorsion considérable du squelette.

3) alors que la phtalocyanine en solution peut être pontée, elle ne l'est pas en phase vapeur.

4) les transitions $\pi \rightarrow \pi^*$ introduites par les azotes aza du pont peuvent être la cause de l'élargissement de la bande de Soret de la phtalocyanine et de la tétraazaporphine.

On discute les polarisations des bandes par rapport au squelette.

Background

Square planar porphyrins and related square planar compounds such as phthalocyanine (Pc), tetrabenzporphin (TBP), and tetrazaporphin (TAP) show an electronic absorption in the visible (Q band) and another in the near uv (B or Soret band). It has long been known that replacement of the metal by two hydrogens, which reduces the symmetry from D_{4h} to D_{2h}, splits these bands into

* Submitted by A.M.S. in partial fulfillment of the requirement for the Ph. D. degree granted by the Department of Chemistry, University of Washington.

** Present address: see end of paper.

four components Q_x, Q_y, B_x, B_y [1]. The splitting is quite different for the Q and B regions; it varies very greatly among the four skeletons listed; and for the Q band of H_2Pc (free base phthalocyanine), it differs considerably between solution and vapor phase [1, 2].

The location of the free base protons has been the subject of long debate. Proposed structures are: (i) two pyrrole and two aza groups, which we shall refer to as *bonded*; (ii) shared protons, which we shall refer to a *bridged*; (iii) hydrogen bonded models somewhere between. Finally we note that *x*-ray work has shown that there can be substantial D_{2h} skeletal distortion in the free base. The purpose of this paper is to use the extended Hückel (EH) model to explore the effect of proton location and skeletal distortion on the free base spectrum.

Various theoretical studies of the free base problem have been undertaken using the self-consistent molecular orbital Pariser-Parr-Pople (SCMO–PPP) method [3, 4]. The more recent studies [3b, 4] correctly predict the magnitude of the Q_x, Q_y splitting in free base porphin (H_2P) and indicate a wider B_x, B_y splitting than was believed earlier [1]. Simple Hückel calculations have been made on phthalocyanine [5], and using this model Chen [6] explicitly considered the effect of bonded and bridged protons on the phthalocyanine spectrum. He concluded that the protons were bridged. However, we believe that Chen chose somewhat arbitrarily the α and β values for the bridged case. This paper draws its inspiration from Chen's work. But here we use the extended Hückel model to study the problem. Moreover, as we shall see, we find that small D_{2h} skeletal distortions can have effects on $Q_x - Q_y$ splitting comparable to the bridged hydrogens.

Finally we note that there is considerable experimental interest in the H_2Pc crystal primarily because of its photoconductivity both in the ir and visible regions [7, 8]. Consequently, attempts have been made to calculate the band structure of this crystal [9, 10] in order to test the theories of production of charge carriers and their mode of transport. However, a knowledge of the molecular wavefunction is required to calculate the band structure of the excess electrons and holes. Sukigara and Nelson [9] used a PPP wavefunction of bonded H_2Pc while Chen [10] has used his Hückel wavefunction for the bridged model of H_2Pc. As we shall show, our extended Hückel calculations provide some important cautions for crystal calculations.

Although Hückel and extended Hückel models have been used to calculate spectra [6, 11], there is an intrinsic difficulty with a one electron model. It is long known [1] that the Q and B states of porphyrins are not single electron transitions but are based on the transitions $a_{2u}(\pi) \rightarrow e_g(\pi^*)$ and $a_{1u}(\pi) \rightarrow e_g(\pi^*)$ heavily mixed together by two electron terms. This mixing decreases in the order $H_2P > H_2TAP \sim H_2TBP > H_2Pc$, where the Q bands are reasonably closer to purer one electron transitions. Yet we shall ignore two electron terms and interpret the $Q_x - Q_y$ splitting simply in terms of the energy gap between $b_{2g}(\pi^*)$ and $b_{3g}(\pi^*)$ [the labels for the two $e_g(\pi^*)$ orbitals in D_{2h} symmetry]. Now we might note that the EH model does not always predict the energy gap between the top filled orbitals $b_{1u}(\pi)$ and $a_u(\pi)$ [D_{2h} labels] in accord with more exact SCMO–PPP calculations or with deduction from experiment. However, we believe that calculations of the splitting of $e_g(\pi^*)$ by D_{2h} distortion will be more

successful since symmetry forces the $e_g(\pi^*)$ orbitals to be degenerate in the metal case; thus, all we ask from the EH model is to correctly predict the effect of the D_{2h} perturbation.

While the EH model may be expected to be qualitatively correct, detailed quantitative agreement is not to be expected. However, our aim here is to throw some new light on the extensive spectral and crystallographic studies that have been done on free base systems. Moreover we are encouraged by the fact that EH calculations used judiciously have in the past made fairly accurate predictions about molecular geometry of porphyrin systems [12].

The EH program used for most of these calculations has been previously described [11].

Free Base Porphin

The crystal structures of free base porphyrins have been extensively studied. We did calculations based on three sets of x-ray coordinates: Coordinates I are D_{4h}, based on tetragonal H_2TPP (free base tetraphenyl porphin) determined by Hamor, Hamor, and Hoard [13]; coordinates II are D_{4h}, based on H_2P (free base porphin) of Webb and Fleischer [14]; coordinates V are D_{2h} based on triclinic H_2TPP studied by Silvers and Tulinsky [15]. (The D_{2h} and D_{4h} labels refer to the carbon-nitrogen skeleton.) The crystal symmetry of these molecules requires tetragonal H_2TPP to have four equivalent pyrrole rings, triclinic H_2TPP to have a center of inversion, while H_2P has no required molecular symmetry. Recent work by Chen and Tulinsky [16] indicates that H_2P may be closer to the D_{2h} structure of triclinic H_2TPP than to the D_{4h} structure earlier reported [14]. As a result we have calculated two structures closely related to II: coordinates III were obtained from II by moving the pyrrole nitrogens farther from the center and the aza nitrogens closer; coordinates IV were obtained with the reverse distortion. Case III corresponds to the type of distortion found for H_2TPP [15] and indicated for H_2P [16].

It is clear from the evidence in all studies that the central H atoms are localized on a diagonally opposed pair of N atoms with a bond distance in the range 0.90 to 0.95 Å. Fig. 1 gives a generalized atom numbering scheme for D_{4h} skeletons and skeletons with D_{2h} distortions which have planes of symmetry passing through the central nitrogens. The numbers 1 and 8 can be either H or C atoms depending on the molecule. Likewise atom number 5 can be either C or N, while atom 4 does not occur in the aza molecules. The planar porphin coordinates found for the three different crystal structures are presented in Table 1. Since the N–H bond distance is the least accurately determined, a range of values to reasonable changes of the N–H distance. For a given set of coordinates, changing the N_9–H_{20} bond distance by 0.05 Å does not reverse the order of the top filled and lowest empty MO's and does not change the energy of any MO by more than 0.015 eV.

An MO energy level diagram for free base porphin with coordinates I, II, and V is given in Fig. 2. To illustrate the effect of the central hydrogens, the energy level pattern of Zn porphin [11] is also included. Comparison with ZnP shows that the four orbitals responsible for the visible and near uv absorption intensity

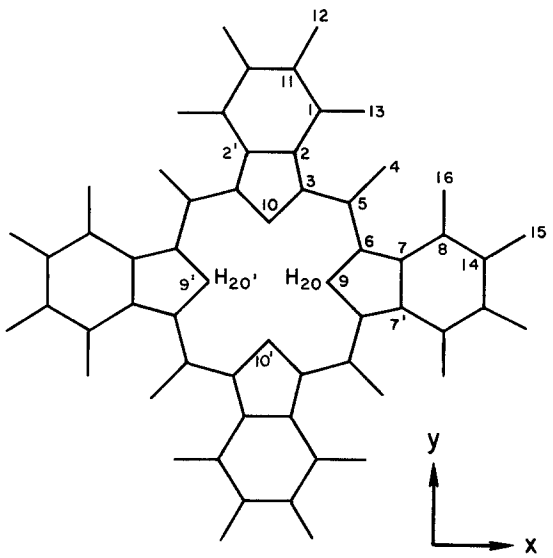

Fig. 1. Skeletal numbering for D_{4h} calculations and D_{2h} distortions preserving x, y symmetry axes

Table 1. Coordinates (x, y) for various Fig. 1 skeletons in Å

Atom	I(D_{4h})[a]		II(D_{4h})[b]		V(D_{2h})[c]		VI(D_{4h})[d]		XIII(D_{4h})[e]		XVIII(D_{4h})[f]	
	x	y	x	y	x	y	x	y	x	y	x	y
1 (H, C)	1.325	5.084	1.309	5.104	1.317	5.111	1.390	5.335	1.394	5.429	1.445	4.888
2 (C)	0.681	4.217	0.671	4.233	0.674	4.244	0.695	4.131	0.695	4.219	0.681	4.120
3 (C)	1.098	2.839	1.104	2.858	1.092	2.849	1.098	2.692	1.098	2.839	1.085	2.692
4 (H_5)	3.208	3.208	3.184	3.184	3.176	3.218			3.208	3.208		
5 (C, N)	2.444	2.444	2.420	2.420	2.430	2.440	2.387	2.387	2.444	2.444	2.387	2.387
6 (C)	2.839	1.098	2.858	1.104	2.897	1.121	2.692	1.085	2.839	1.098	2.692	1.085
7 (C)	4.217	0.681	4.233	0.671	4.254	0.678	4.131	0.695	4.219	0.695	4.120	0.681
8 (H, C)	5.084	1.325	5.104	1.309	5.180	1.233	5.334	1.390	5.429	1.394	4.888	1.445
9 (N)	2.054	0.000	2.053	0.000	2.100	0.000	1.910	0.000	2.054	0.000	1.910	0.000
10 (N)	0.000	2.054	0.000	2.053	0.000	2.030	0.000	1.910	0.000	2.051	0.000	1.910
11 (C)							0.695	6.539	0.695	6.639		
12 (H)							1.235	7.474	1.237	7.578		
13 (H)							2.470	5.335	2.478	5.429		
14 (C)							6.539	0.695	6.639	0.695		
15 (H)							7.474	1.235	7.578	1.237		
16 (H)							5.335	2.470	5.429	2.478		
20 (H)	1.104	0.000	1.103	0.000	1.150	0.000	0.960	0.000	1.104	0.000	0.910	0.000

[a] Tetragonal H_2TPP [13]. The D_{4h} label refers to symmetry of carbon-nitrogen skeleton.
[b] H_2P [14].
[c] Triclinic H_2TPP [15].
[d] H_2Pc, average of Robertson's D_{2h} coordinates [21].
[e] H_2TBP, derived from coordinates I.
[f] H_2TAP, derived from coordinates VI.

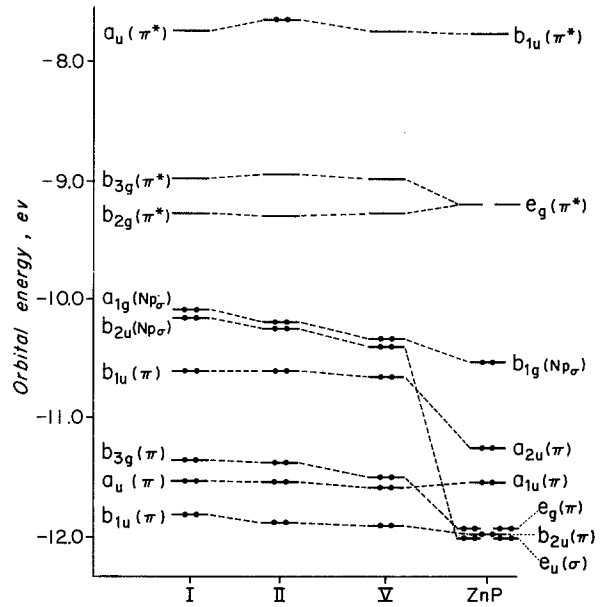

Fig. 2. Top filled and lowest empty MO's of H_2P and ZnP. For full geometry see Table 1

changes as follows: One $e_g(\pi^*)$ of ZnP rises in energy while the energy of the other goes down a bit; $a_{2u}(\pi)$ rises in energy while the energy of $a_{1u}(\pi)$ stays fixed. The energy splitting of the orbitals $b_{2g}(\pi^*)$ and $b_{3g}(\pi^*)$ is that expected by perturbation theory: $b_{2g}(\pi^*)$, which has non-zero coefficients on the pyrrole nitrogens, is at lower energy than is $b_{3g}(\pi^*)$, which has non-zero coefficients on the aza nitrogens. That $a_{1u}(\pi)$ is unaffected is also expected, since it has zero coefficient on all central nitrogens. However the shift of $a_{2u}(\pi)$ to higher energy is not necessarily expected. It also occurs in SCMO–PPP calculations, when free base is compared to metalloporphin [3].

The energy level diagram also indicates the presence of two low lying $n \rightarrow \pi^*$ transitions, including the symmetry allowed $b_{3u}(\sigma) \rightarrow b_{2g}(\pi^*)$. Although these are predicted to be in the near ir, our EH calculations generally underestimate the energy of charge transfer transitions [17]. Consequently, the allowed $n \rightarrow \pi^*$ transition may appear in the Soret region and be obscured by stronger $\pi \rightarrow \pi^*$ bands, a possibility suggested by Sundbom [4] on the basis of theoretical work and by Antenson [18] who, on the basis of the sharpness of Q_x at low temperature, concluded that Q_x is the lowest singlet state.

Although it is reasonably clear that the H atoms in free base porphyrins are bonded, EH calculations on the bridged model are useful for comparison purposes. The N–H bond distance was varied from 1.45 to 1.53 Å. In this configuration there are four equivalent N atoms and the D_{2h} perturbation due to H atoms is much less severe. The π electron system is essentially D_{4h}; therefore, it is not surprising that the splitting of the lowest empty $e_g(\pi^*)$ orbitals is only about 16 cm^{-1}.

Table 2. Calculated and experimental values of Q_x, Q_y and Δ for free base porphins

Coordinates[a]	Q_x (cm^{-1})	Q_y (cm^{-1})	Δ[b] (cm^{-1})
I (D_{4h}, H_2TPP)	11190	13580	2390
II (D_{4h}, H_2P)	10520	13190	2660
III (D_{2h}, H_2P)[c]	10400	12790	2390
IV (D_{2h}, H_2P)[d]	10630	13560	2930
V (D_{2h}, H_2TPP)	11110	12790	1680
H_2P (vapor, 393° C)	15930[e]	19550	3610
H_2P (benzene, 25° C)	16200	19200	3000
H_2TPP (vapor, 448° C)	15060	18310	3250
H_2TPP (oil, 304° C)	15200	18100	2900
H_2TPP (oil, 30° C)	15400	18320	2830
H_2TPP (benzene, 25° C)	15380	18250	2860

[a] See Table 1 for full geometry.

[b] The calculated value is the $b_{3g}(\pi^*) - b_{2g}(\pi^*)$ energy gap while the experimental value is the $Q_x - Q_y$ splitting.

[c] Identical to II except with N(9): $x = 2.083$, $y = 0$ and N(10): $x = 0$, $y = 2.023$.

[d] Identical to II except with N(9): $x = 2.023$, $y = 0$ and N(10): $x = 0$, $y = 2.083$.

[e] All experimental values from Ref. [19].

Because of the contribution of two electron terms, it is naive to interpret the experimental splitting of the Q_x and Q_y bands in terms of the energy difference Δ between the empty orbitals $b_{2g}(\pi^*)$ and $b_{3g}(\pi^*)$. Nonetheless since the observed splitting and calculated Δ both arise from the lifting of the D_{4h} degeneracy, we believe they should be qualitatively correlated. Thus when the bridged model gives $\Delta = 16\ cm^{-1}$, as just mentioned, we believe that a splitting of this order of magnitude would be expected for a real molecule with this structure.

Table 2 gives calculated transition energies $b_{1u}(\pi) \rightarrow b_{2g}(\pi^*)$, $b_{3g}(\pi^*)$ for several skeletal geometries, the splitting values Δ, and the experimental values [19]. The calculated Δ values are comparable to experimental. There are marked changes of calculated Δ with changes in the carbon-nitrogen skeleton. Experimentally Δ changes with substituents, with temperature, and in going from solution to vapor. We believe that some of the effect of substituent and all of the effect of temperature and phase change should be attributed to changes in the carbon-nitrogen skeleton.

Although we are confident that observed changes in $Q_x - Q_y$ splitting can be related to changes in the carbon-nitrogen skeleton, because of the crudity of the model, the relation of particular geometries to particular experimental conditions is on less firm ground. We note that calculated values of Δ are higher using H_2P rather than H_2TPP geometry, consistent with experiment. Chen and Tulinsky's [16] recent work on H_2P indicates that the pyrrole nitrogens are separated by a greater distance than the aza nitrogens. This result plus chemical intuition suggests that the change in $Q_x - Q_y$ splitting that occurs in going from solution to vapor is due to a change such as from coordinates III to coordinates II. That is, in solution the carbon-nitrogen skeleton is D_{2h} with pyrrole nitrogens moved farther from the center and aza nitrogens moved closer. However in vapor, we propose that thermal motion causes the free base porphyrin to take on a more geometrically symmetrical configuration.

Other spectral correlations might be mentioned. The low energy transition $b_{1u}(\pi) \rightarrow b_{2g}(\pi^*)$ is predicted to be polarized along the x axis; consequently, the Q_x band should be polarized along the proton axis. This agrees with the results from the polarization reflection studies of Anex and Umans [20]. It is also interesting to note that the EH model correctly predicts the Q_y band to be more intense than the Q_x band. This result is a consequence of the fact that both $b_{1u}(\pi)$ and $b_{3g}(\pi^*)$ are strongly localized on N_{10}.

Free Base Phthalocyanine

In a classical two-dimensional analysis Robertson [21] determined the x-ray structure of free base phthalocyanine. Although the experimental uncertainty of ± 0.03 Å is large by today's standards, the carbon-nitrogen skeleton is most likely D_{2h}. Robertson, however, did not directly observe the inner protons. There are two possible bonding schemes for these H atoms. They can be bonded directly to two of the four nitrogen atoms, or each hydrogen can be shared by two neighboring nitrogens.

The position of the central hydrogens is still a matter of some controversy. Both proponents of the bridged and bonded model have used experimental evidence to buttress their conclusions. Fleischer [22] has performed a refinement on Robertson's original data and has concluded that the hydrogens are in a bridged position. This view is supported by Berezin [23] who proposed a model in which the internally dissociated protons are shared by six nitrogen atoms. Sharp and Landon [24] also used the bridged H model to characterize the spectroscopic properties of a new polymorph of H_2Pc. From a neutron diffraction study of H_2Pc, however, Hoskins, Mason, and White [25] have found evidence of four half-hydrogens which lie very nearly on a line which join centrosymmetrically related pyrrole nitrogen atoms. Gurinovich [26], studying the N–H stretching frequency in a variety of porphyrin type compounds, found that as the molecule becomes more complicated the value of ν(N–H) decreases. This suggested to him that the shift of ν(N–H) of H_2Pc relative to H_2P is not due to intramolecular H bonding. Although Hoskins *et al.* make a compelling argument for the bonded model in H_2Pc crystals, there is no reason to believe that the H atom position is the same in solution, vapor, and crystal. Thus, calculations were performed for both bonded and bridged models.

a) Bonded Model

The coordinates for the bonded model are given in Table 1 using the numbering of Fig. 1: coordinates VI are a D_{4h} average of the D_{2h} values obtained by Robertson. Coordinates VII and VIII were obtained from VI by moving the pyrrole nitrogen atoms farther apart by 0.02 Å (VII) and 0.05 Å (VIII). The aza nitrogens were moved closer together by the same amount for each case. The NH bond distance was set at 0.95 Å, and variation of this value over ± 0.05 Å had little effect on the result.

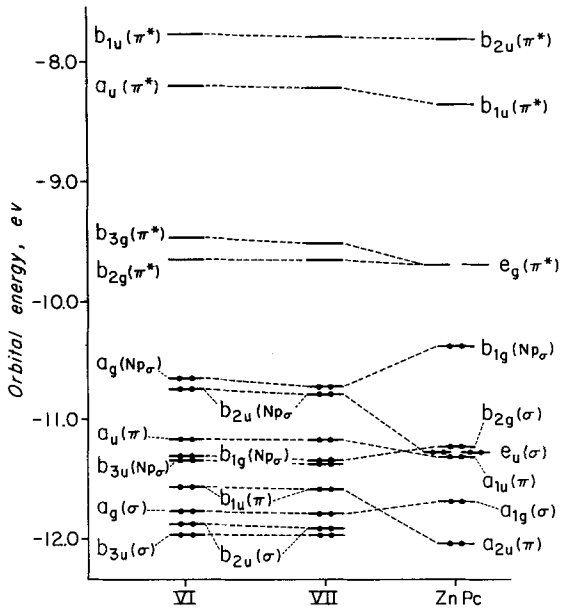

Fig. 3. Top filled and lowest empty MO's of bonded H_2Pc and ZnPc. For full geometry see Table 1

An MO energy level diagram for H_2Pc with coordinates VI and VII is given in Fig. 3 along with ZnPc [17b]. Comparison with ZnPc shows that free base formation affects the four orbitals responsible for the visible and near uv absorption intensity in a very similar manner as in porphin, Fig. 2: The orbital $b_{3g}(\pi^*)$, with non-zero coefficients on the aza nitrogens, is at higher energy than $b_{2g}(\pi^*)$ with non-zero coefficients on the pyrrole nitrogens. Also the orbital $a_{2u}(\pi)$ in ZnPc rises strongly in energy while $a_{1u}(\pi)$ only rises slightly. The latter, as in porphin, has nodes at the central nitrogen atoms.

One important difference between ZnP and ZnPc, as shown by SCMO–PPP calculations, is that in ZnP the top filled orbitals $a_{1u}(\pi)$ are very close in energy while in ZnPc $a_{2u}(\pi)$ is far lower in energy than $a_{1u}(\pi)$. In ZnPc the Q bands are basically one electron transitions $a_{1u}(\pi) \rightarrow e_g(\pi^*)$. Although free base formation causes $a_{2u}(\pi)$ to rise in energy relative to ZnPc, we believe that in H_2Pc the Q bands will still be due to transitions $a_u(\pi) \rightarrow b_{2g}(\pi^*)$, $b_{3g}(\pi^*)$. In this case the lower energy Q_x band will be polarized perpendicular to the H–H axis while in H_2P it is polarized parallel to the H–H axis[1,2].

Table 3 gives the calculated values of Q_x and Δ for coordinates VI, VII, and VIII plus the corresponding experimental results [2]. The transition energies of

[1] In this paper we follow the general convention that refers to the lower energy Q band as Q_x and upper one Q_y, without implying an absolute orientation. The reader should note in each case the polarization predicted. (We note that in chlorophyll the reduced ring is conventionally placed on the x axis forcing the protons on the y axis and making the lower energy band y polarized. For this reason it is generally called Q_y.)

[2] *Note Added in Proof:* Recent PPP calculations by M. Sundborn (Ph. D. Thesis) predict the lower energy Q_x band is polarized parallel the H–H axis, contrary to what the extended Hückel calculations suggest.

Table 3. Calculated and experimental values of Q_x, Δ, and the polarization for various geometries of free base phthalocyanine

Geometry[a]	Coordinates H_{20} (x, y)	Q_x (cm^{-1})	Δ (cm^{-1})	Polarization[b]
VI	0.960, 0.000	12310	1440	y
VII[c]	0.970, 0.000	12430	1270	y
VIII[d]	0.985, 0.000	12560	1120	y
IX	1.081, 0.000	13090	−17	x(L)
IX	1.910, 0.000	13460	88	y(M)
IX	2.110, 0.000	13280	374	y(M)
IX	2.426, 0.000	13090	761	y(M)
X	1.380, 0.000	13100	72	M
X	2.030, 0.000	13300	335	M
X	2.210, 0.000	13160	612	M
X	0.000, 1.325	12990	242	M
XI	1.830, 0.000	13340	480	M
XI	1.977, 0.000	13150	632	M
XII	1.030, 0.000	12690	577	M
XII	1.830, 0.000	13090	582	M
XII	2.030, 0.000	13020	819	M
XII	2.21, 0.000	12880	1120	M
XII	0.000, 1.775	13260	617	M
XII	0.000, 2.110	13370	197	M
H_2Pc in CLNP Ref. [43]		14330	730	
H_2Pc vapor Ref. [2a]		14580	1490	

[a] Full geometry given in Tables 1 and 4.
[b] Polarization of lowest energy Q band given with respect to axes, Figs. 1 and 4; x(L) refers to bridged structure with D_{4h} carbon-nitrogen skeleton.
[c] Identical to VI (bonded H_2Pc) except N_9: $x = 1.92$, $y = 0$; N_{10}: $x = 0$, $y = 1.90$.
[d] Identical to VI except N_9: $x = 1.935$, $y = 0$; N_{10}: $x = 0$, $y = 1.885$.

the EH model should more properly be compared to the average of the excited singlet and triplet energies than to the excited singlets alone. Although phosphorescence of H_2Pc has not been observed, results for metal phthalocyanines [27] indicate that the triplet should be in the region 9000 to 10000 cm^{-1}. When this is averaged in with the observed singlet, the result agrees reasonably well with the EH transition energy. The difference in energy Δ between $b_{2g}(\pi^*)$ and $b_{3g}(\pi^*)$ corresponds quite well to the energy gap between Q_x and Q_y observed in vapor but tends to be larger than the gap observed in solution, as shown in Table 3.

b) Bridged Model

The coordinates of the bridged model are given in Table 4 using the numbering of Fig. 4. The following coordinates were used: Coordinates IX form the same D_{4h} carbon-nitrogen skeleton as VI; coordinates X are the D_{2h} carbon-nitrogen coordinates reported by Robertson [21]; coordinates XI and XII are slight variants of X with bond lengths and angles within Robertson's experimental error. Unlike the bonded model, the proper distance of the central hydrogens from the nitrogens is not apparent. Moreover in the D_{2h} model the distance

Table 4. Coordinates (L, M) for various Fig. 4 skeletons in Å

Atom	IX (D_{4h})[a]		X (D_{2h})[b]		XI (D_{2h})[c]		XII (D_{2h})[c]		XX (D_{2h})[d]	
	L	M	L	M	L	M	L	M	L	M
1 (H, C)	2.789	4.755	2.75	4.77	2.726	4.772	2.726	4.772	2.595	4.496
2 (C)	2.429	3.412	2.41	3.42	2.404	3.422	2.390	3.422	2.415	3.419
3 (C)	1.136	2.671	1.145	2.64	1.141	2.642	1.136	2.642	1.145	2.640
5 (C, N)	0.000	3.376	0.000	3.32	0.000	3.32	0.000	3.316	0.000	3.320
6 (C)	2.671	1.136	2.71	1.13	2.704	1.139	2.704	1.139	2.710	1.130
7 (C)	3.412	2.429	3.405	2.45	3.405	2.458	3.390	2.458	3.386	2.458
8 (H, C)	4.755	2.789	4.73	2.84	4.745	2.840	4.745	2.840	4.448	2.671
9 (N)	1.351	1.351	1.38	1.325	1.380	1.325	1.380	1.325	1.380	1.325
10 (C, N)	3.376	0.000	3.43	0.000	3.430	0.000	3.430	0.000	3.430	0.000
12 (H)	2.026	5.519	1.974	5.52	1.950	5.520	1.950	5.520		
13 (C)	4.132	5.115	4.08	5.17	4.081	5.154	4.081	5.154		
14 (H)	4.412	6.158	4.341	6.217	4.342	6.201	4.342	6.201		
15 (C)	5.115	4.132	5.07	4.20	5.081	4.190	5.081	4.190		
16 (H)	6.158	4.412	6.117	4.498	6.128	4.488	6.128	4.488		
17 (H)	5.519	2.026	5.506	2.09	5.521	2.090	5.521	2.090		
20 (H)	0.68–2.426	0.000	0.68–2.21	0.000	1.03–1.975	0.000	0.53–2.21	0.000	1.830	0.000

[a] H_2Pc, D_{4h} average of [21], a rotation of coordinates VI.
[b] H_2Pc, Ref. [21].
[c] H_2Pc, slight distortion of coordinates X.
[d] H_2TAP, derived from coordinates X.

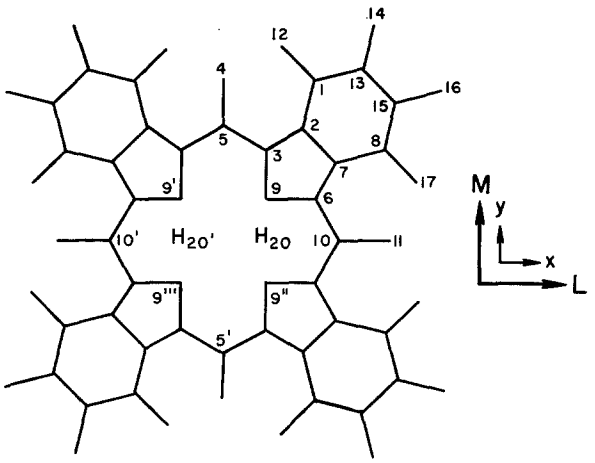

Fig. 4. Skeletal numbering for bridged models and D_{2h} distortions preserving L, M symmetry axes. For D_{2h} distortion, Robertson [21] found the N_9–$N_{9'}$ distance to be 2.76 Å and the N_9–$N_{9''}$ distance to be 2.65 Å

between N_9 and $N_{9'}$ is 2.76 Å while the N_9–$N_{9''}$ distance is 2.65 Å. It is not clear whether the H atoms belong on the M axis between N_9–$N_{9'}$ or on the L axis between N_9–$N_{9''}$. Accordingly we varied the distance of the hydrogens from the center, and in the D_{2h} geometry the axis upon which they were placed.

Table 3 gives the energy gap $b_{3g}(\pi^*) - b_{2g}(\pi^*) \equiv \Delta$ for different carbon-nitrogen skeletons and various distances of the protons from the center. More values are given in Ref. [17b]. For a D_{4h} carbon-nitrogen skeleton (IX), $|\Delta|$ is under 100 cm^{-1} until the distance between central hydrogen and bridged nitrogen is under ~ 1.3 Å. As the distance between the central hydrogens and bridge nitrogens decreases, the energy of $b_{3g}(\pi^*)$ rises above $b_{2g}(\pi^*)$ exactly as in bonded H_2Pc. To reach $\Delta \sim 730\ cm^{-1}$, corresponding to the observed solution $Q_x - Q_y$ splitting, this distance has to be reduced to 0.95 Å.

For the D_{2h} model, Δ depends on the specific carbon-nitrogen geometry, the position of the central hydrogens, and the axis upon which these hydrogens are placed. For the carbon-nitrogen skeletons studied and for the hydrogen distance from the center varying from 0.68 Å to 2.43 Å we have obtained Δ values between $-270\ cm^{-1}$ and $+1120\ cm^{-1}$. We have done calculations on NiPc using D_{2h} coordinates XII and obtained a splitting of 400 cm^{-1} [28]. It would seem, then, that if the distance of the hydrogen atoms from the bridged nitrogens is larger than ~ 1.3 Å, the primary cause for any significant Δ value is the D_{2h} distortion of the carbon-nitrogen skeleton. *Therefore to obtain the experimental Δ value of 730 cm^{-1} from a bridged model, either there is an incipient* NH *bond with the bridge nitrogens or there is substantial D_{2h} distortion of the carbon-nitrogen skeleton.*

The energy level pattern for different geometries of the bridged model are given in Fig. 5. As in the bonded model (*vide ante*) we interpret the two Q bands as $a_u(\pi) \rightarrow b_{2g}(\pi^*)$, $b_{3g}(\pi^*)$. If the splitting of $b_{2g}(\pi^*)$, $b_{3g}(\pi^*)$ is due to incipient bond formation between the central hydrogens and bridge nitrogens, then as in the

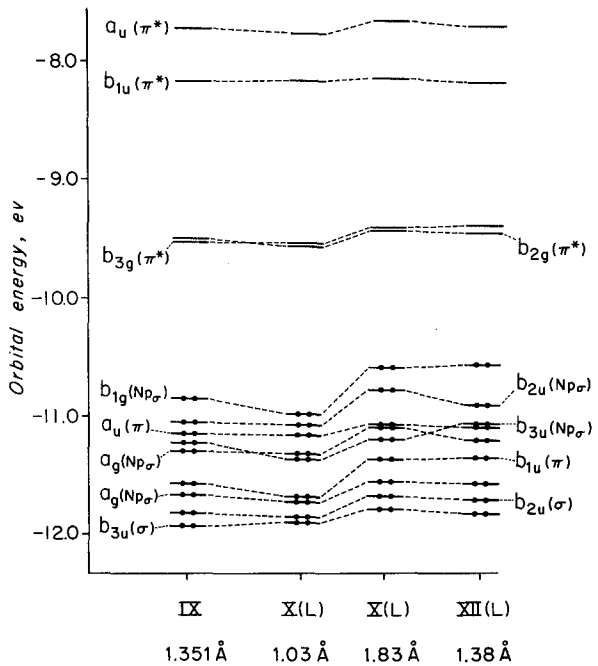

Fig. 5. Top filled and lowest empty MO's for bridged H_2Pc. The coordinates and distance of the hydrogens from the center are given. Full geometry may be found in Table 4

bonded model, the orbital $b_{2g}(\pi^*)$ with non-zero coefficients on the bonded nitrogens will be at lower energy and the lower energy transition will be polarized perpendicular to the H–H axis. In Fig. 4, if the splitting is due to incipient NH bond formation, placing the hydrogens on the L axis makes the lower energy transition polarized parallel to M. The Robertson distortion shown in Fig. 4 also tends to put $b_{2g}(\pi^*)$ at lower energy than $b_{3g}(\pi^*)$, so that if the protons are placed on the L axis of the D_{2h} model the two effects cooperate to enhance splitting. Our calculations suggest that the experimental splitting of 730 cm^{-1} can be obtained from the Robertson distortion alone, from incipient NH bond formation alone, or from both effects acting cooperatively. For the effects to act cooperatively, the hydrogen atoms must be on the L axis of the Robertson carbon-nitrogen skeleton in Fig. 4.

There are three geometric parameters which significantly influence the calculated results in bridged H_2Pc with D_{2h} skeletal symmetry. From the results of free base tetrazaporphin calculations (*vide infra*), it will be seen that the most important of these is the coordinates of the atoms in the inner ring: C_3, N_5, C_6, N_9, and N_{10}. Another factor, although less important, is the inclination of the benzene rings toward the M molecular axis. When calculations were done for a constant set of inner ring coordinates, Δ increases as the benzene rings were foreshortened in the M direction. The final parameter, which has already been discussed in detail, is the position of the central hydrogen atoms.

c) Postion of $n-\pi^*$ Transitions

In normal phthalocyanine solution spectra, the half-widths of the Q and B bands are approximately 400 and 5000 cm^{-1} respectively. Hochstrasser and Marzzacco [29] have proposed that the presence of $n\rightarrow\pi^*$ transitions, even though forbidden, under allowed $\pi\rightarrow\pi^*$ transitions broadens the latter. Although the MO diagrams for both bonded (Fig. 3) and bridged (Fig. 5) indicate the possibility of $n\rightarrow\pi^*$ transitions under both the Q and B bands, only the B shows temperature independent broadening. However, Fielding and MacKay [30, 31], in a study of the single crystal absorption of H_2Pc, observed weak transitions not split by the crystalline field in the 4000 to 10000 cm^{-1} region. Since the extinction coefficients of these bands are larger than those usually associated with singlet-triplet transitions, Fielding and MacKay assigned them to symmetry forbidden transitions which should be allowed to some extent in a single crystal. Although we do predict $n\rightarrow\pi^*$ transitions in this region, the strong fluorescence of H_2Pc suggests that no other singlets lie under the first $\pi\rightarrow\pi^*$ transition. In addition, our EH method generally underestimates the energy of $n-\pi^*$ transitions [17].

d) Relation to Experimental Spectra

Before attempting to summarize our conclusions, let us list some of the pertinent spectral behavior of H_2Pc [2]. (1) There is a strong variation in the Q_x-Q_y splitting which is more environment than temperature dependent. For example, in silicone oil over the temperature range 297° K to 577° K the splitting varies only from 730 to 770 cm^{-1}. (2) In going from solution to vapor Q_y is blue shifted about 1000 cm^{-1} while Q_x is blue shifted normally (about 250 cm^{-1}). (3) The Q_y band shows anomalous broadening with temperature although the relative Q_x, Q_y intensities are preserved. This latter effect has tentatively been attributed to vibronic coupling between the Q_x, Q_y states [2a].

From the results of our calculations we can suggest three structural changes to account for the striking increase in Q_x-Q_y splitting on going from vapor to solution:

(1) Both structures are bonded. In vapor the carbon-nitrogen skeleton is D_{4h} and in solution D_{2h}, with the pyrrole nitrogens more separated than the aza nitrogens.

(2) Both structures are bridged. In the vapor the total splitting results from cooperation between a D_{2h} Robertson type distortion and incipient bond formation between central hydrogen and bridged nitrogen.

(3) In solution H_2Pc is bridged, most likely with a Robertson D_{2h} distortion with protons on the L axis, while in the vapor H_2Pc is bonded, most likely with D_{4h} carbon-nitrogen skeleton.

Which of these three explanations is most likely? Our bridged calculations of Δ include a range that readily encompasses the observed solution Q_x-Q_y splitting of ~ 700 cm^{-1}. They are never as large as the ~ 1500 cm^{-1} vapor splitting, and they only approach this value with central hydrogens essentially bound to the bridged nitrogens. Since such a bond seems chemically unreason-

able, *we rule out a bridged structure for the vapor* and reject explanation (2). However our bonded calculation of Δ give values as low as 1100 cm^{-1}, and conceivably 700 cm^{-1} could be achieved. Thus though our calculations indicate explanation (3), the inaccuracy of our method prevents us from ruling out explanation (1).

A great amount of work has been done on crystal and film H_2Pc. Our calculations on the bridged model show that values of Δ comparable to experiment lead to a lower energy band polarized parallel to M axis. Lyons, Walsh, and White [32] obtained better agreement between the experimental polarized spectra of single crystal of β–H_2Pc and spectra calculated using a point dipole approximation if they assumed the lower energy transition is polarized along the L axis. Their conclusion, however, is not completely unambiguous, for there is great difficulty in even correctly assigning the transitions in crystal spectra. Lucia and Verderame [33] observed that the Δ of thin films of β–H_2Pc is approximately the same as the vapor, and they have suggested that the Q_x and Q_y states are each red-shifted by about 600 cm^{-1} in the crystal site then split by about 200 to 500 cm^{-1} under the factor group (Davydov splittings). This explanation seems to imply that the structure of the free base in the vapor closely resembles that in the crystal, and it is the solution results that are anomalous. Sharp and Landon [24] have stated that the spectra of thin films of α–H_2Pc should be most closely related to solution spectra since the α-form is a metastable and less ordered polymorph than the usually studied β–H_2Pc. However, the Δ of α–H_2Pc is almost 2000 cm^{-1} which is closer to the vapor rather than the solution results.

Recent X-ray work on metal phthalocyanines [34, 35] indicates that the phthalocyanine skeleton is fairly flexible. Consequently, the phthalocyanine ring geometry may be very sensitive to changes in the molecular environment. The strong dependence of the $Q_x - Q_y$ splitting upon solvent may be a reflection of such geometry changes. Edwards [2] found that Δ is much more environment than temperature dependent. For example, Δ is 699, 767, 870, 909, and 1487 cm^{-1} in HMPA (300° K), 1–CLNP (300° K), Kr (20° K), Ar (20° K), and vapor respectively. These experimental results plus the calculations reported here make clear that "isolated molecule" energies suitable for crystal calculations may be dependent on crystal packing, which can affect the carbon-nitrogen skeletal geometry and in turn the proton positions. It may be that neither the vapor nor the solution $Q_x - Q_y$ split correspond to the "isolated molecule" suitable for a zeroth order wavefunction for a particular solid phase. Since the Davydov splitting for a crystal phase will be comparable to the $Q_x - Q_y$ splitting, which is not clearly known, understanding the crystal spectra of H_2Pc will be difficult. Metallophthalocyanines pose a much simpler problem.

e) Relation to Theory of Chen and Berezin

Using the simple Hückel model, Chen [6] successfully reproduced the observed absorption spectra of H_2Pc with a bridged hydrogen model by slightly raising the Coulomb integral α value of the adjacent bridge nitrogens. Our EH calcu-

lations show that the protons *lower* the α value of the adjacent bridge nitrogens. Moreover they show that unless the hydrogen-bridge nitrogen distance becomes comparable to normal bond lenghts, a carbon-nitrogen skeleton distortion is also necessary if the observed 730 cm^{-1} splitting is to be achieved. We also note that Chen placed the bridged hydrogens on the M axis of the D_{2h} skeleton (Fig. 4), while our calculations show the L axis to be more likely.

Berezin [23] proposed that the internally dissociated H atoms are stabilized in the presence of the negative electrostatic field produced by its two dissociated electrons. Maximum stabilization would therefore probably occur when the proton was situated equidistant from the three N atoms (N_9, $N_{9''}$, and N_{10}). Our calculations show that such geometry gives too small a splitting for a D_{4h} carbon-nitrogen skeleton.

Free Base Tetrabenzporphins

Although work on the X-ray structure of tetrabenzporphin was begun by Robertson [36], no detailed analysis of a TBP has been published. It was therefore necessary to make some assumptions about the structure of H_2TBP on the basis of what is known about other free bases. Coordinates XIII (Table 1) are derived from the H_2TPP D_{4h} coordinate of Hamor, Hamor, and Hoard [13] with C_2–C_2' and C_7–C_7' increased to 1.39 Å so that the outer benzo rings can achieve the normal hexagonal benzene geometry. Coordinates XIV and XV were obtained from XIII by moving the pyrrole nitrogens farther apart by 0.06 Å (XIV) and 0.10 Å (XV) and the aza nitrogens closer together by the same amounts respectively. Coordinates XVI are derived from the D_{4h} geometry of H_2Pc, coordinates VI. All these cases are bonded with an NH distance of 1 Å. Coordinates XVII were derived from the bridged D_{2h} coordinates of H_2Pc, XII.

Fig. 6 gives the energy level scheme for ZnTBP [17b] and several geometries of H_2TBP. Unlike ZnP but like ZnPc, the top filled MO is $a_{1u}(\pi)$ a result found by SCMO–PPP calculations [3]. Just as for H_2P and H_2Pc, the effect of free base formation is to raise the lower energy $a_{2u}(\pi)$ of the ZnTBP. We see in Fig. 6 that the order of $a_u(\pi)$, $b_{1u}(\pi)$ (the top filled orbitals of H_2TBP) is dependent on geometry. As shown in Table 5, the splitting of $b_{2g}(\pi^*)$ and $b_{3g}(\pi^*)$ is slightly larger for bonded H_2TBP than for either bonded H_2P or H_2Pc. In bridged H_2TBP the splitting is smaller than in bridged H_2Pc. The larger splitting for bonded H_2TBP is due to greater localization of the $e_g(\pi^*)$ orbitals onto the central nitrogen atoms. For all geometries in Table 5, the splitting Δ is rather larger than the 1395 cm^{-1} $Q_x - Q_y$ splitting given by Solov'ev *et al.* [37]. In addition to this, they observe the B band clearly split into two components, whose separation is 1000 cm^{-1}. This is the only one of the four free bases studied herein that shows clear B band splitting.

The polarization of the transitions relative to the H–H axis is determined by which orbital $b_{1u}(\pi)$ or $a_u(\pi)$ is higher in energy. Because the energies are so close, the neglected two electron terms will be important, and we cannot answer this question within the present model.

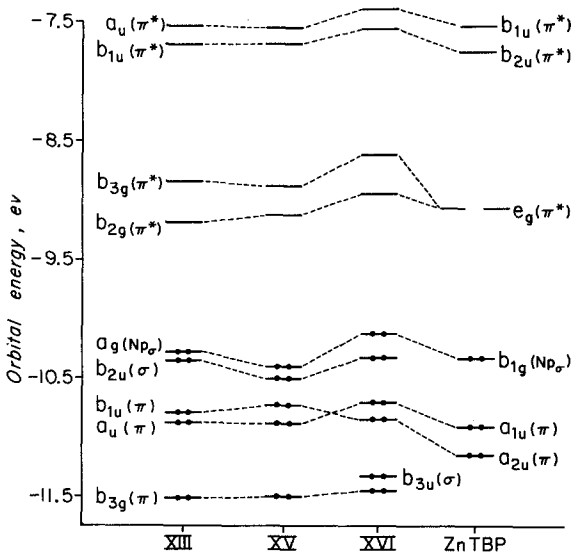

Fig. 6. Top filled and lowest empty MO's of H_2TBP and ZnTBP. Geometry of XIII given in Table 1 while XV and XVI are described in text

Table 5. Calculated and experimental values of Q_x, Δ, and the polarization for various geometries of free base tetrabenzporphin

Geometry	Q_x (cm^{-1})	Δ (cm^{-1})	Polarization
XIII[a]	13020	2663	x
XV[b]	12850	2279	x
XV[c]	12930	1914	x
XVI[d]	14150	2759	y
XVII[e]	14660	99	M
H_2TBP in pyridine Ref. [37]	15020	1395	
H_2TBP in CLNP Ref. [41]	14970	1363	

[a] Bonded H_2TBP, full geometry given in Table 1.
[b] Identical to XIII except N_9: $x = 2.08$, $y = 0$; N_{10}: $x = 0$, $y = 2.02$; H_{20}: $x = 1.08$, $y = 0$.
[c] Identical to XIII except N_9: $x = 2.10$, $y = 0$; N_{10}: $x = 0$, $y = 2.00$; H_{20}: $x = 1.10$, $y = 0$.
[d] Bonded H_2TBP, derived from coordinates VI (Table 1).
[e] Bridged H_2TBP, derived from coordinates XII (Table 4) with H_{20}: $x = 1.83$, $y = 0$.

Free Base Tetrazaporphins

No complete structural analysis of a tetrazaporphin has been published although preliminary investigations have been made on the X-ray structure of various aza substituted porphyrins [36, 38]. There is thus a fairly large uncertainty in the geometry of this molecule; e.g., the central protons in H_2TAP may be either bonded or bridged, while the skeletal geometry may be similar to H_2P, as was assumed in earlier calculations [3a], or it may be more closely related to H_2Pc. Consequently, a fairly wide range of atomic coordinates derived

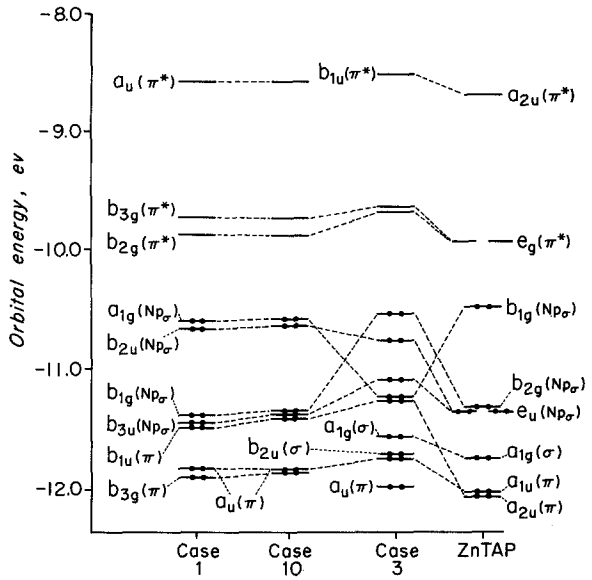

Fig. 7. Top filled and lowest empty orbitals of ZnTAP and H_2TAP. Description of geometry given in Tables 1, 4, and 6

from bonded H_2P, bonded H_2Pc, and bridged H_2Pc were used. Coordinates XVIII (Table 1) were derived from D_{4h} coordinates VI of H_2Pc. Coordinates XIX were derived from D_{4h} coordinates I of H_2TPP. Coordinates XX, XXI, XXII were bridged structures obtained from D_{2h} coordinates X, XI, XII of H_2Pc. Coordinates XXIII have the D_{2h} distortion of the carbon-nitrogen skeleton as in XX, but the central hydrogen atoms are bonded. In all cases the C_2–C_2' and C_7–C_7' bond (C_2–C_7 in bridged model) have the porphin bond distance of 1.362 Å.

Fig. 7 compares the calculated MO's for bonded and bridged H_2TAP with ZnTAP. As in previous cases the $a_{2u}(\pi)$ orbital of ZnTAP rises in energy in the free base. The splitting of the empty orbitals $b_{2g}(\pi^*)$ and $b_{3g}(\pi^*)$ is the same as in the comparable H_2Pc skeletons. In the bonded cases, therefore, the lowest energy Q transition is polarized parallel to the proton axis. In the bridged cases with the H–H axis parallel to L, the same is true. With the D_{2h} carbon-nitrogen skeleton XX and the H–H axis parallel to M, a negligible splitting occurs. The polarization predicted for the bonded cases agrees with that predicted by SCMO–PPP calculations [3] and is like H_2P. As in H_2Pc, there is a fairly large number of $n \rightarrow \pi^*$ transitions predicted to be in the region of the Q and B bands. If we again assume that we have underestimated the energy of these transitions, the diffuseness of the B and N bands in H_2TAP [39, 40] may be caused by these underlying $n \rightarrow \pi^*$ transitions.

Table 6 compares the calculated values of Q_x and for various geometries of H_2TAP with experimental results. Comparing these values with those in Table 3, one finds that the calculated splitting for bonded H_2TAP is less than that for bonded H_2Pc with a similar geometry, but the reverse is true for bridged H_2Pc

Table 6. Calculated and experimental value of Q_x and Δ for various geometries of free base tetrazaporphins

Case	Geometry	Coordinates H_{20} (x, y)	Q_x (cm^{-1})	Δ (cm^{-1})	Polarization
1	XVIII[a]	0.91, 0.000	12740	1110	x
2	XIX[b]	1.054, 0.000	9530	1085	x
3	XX[c]	1.83, 0.000	13030	295	L
4	XX	0.000, 1.83	13020	10	L
5	XXI[d]	1.03, 0.000	14830	553	L
6	XXI	1.83, 0.000	12840	653	L
7	XXII[e]	1.83, 0.000	12840	819	L
8	XXII	2.03, 0.000	12130	1144	L
9	XXII	2.21, 0.000	11510	1522	L
10	XXIII[f]	0.695, 0.667	12480	1193	[g]
11	XXIII	0.900, 0.505	12640	1121	[g]
H_2TAP in pyridine Ref. [39]			16030	1960	
H_2TAP in chlorobenzene Ref. [40]			16210	2140	

[a] Bonded H_2TAP, derived from geometry VI. Full coordinates given in Table 1.
[b] Bonded H_2TAP, derived from geometry I.
[c] Bridged H_2TAP, derived from geometry X. Full coordinates given in Table 4.
[d] Bridged H_2TAP, derived from geometry XI.
[e] Bridged H_2TAP, derived from geometry XII.
[f] Geometry of carbon-nitrogen skeleton same as XX, but central hydrogen atoms are bonded.
[g] Polarization parallel to axis connecting pyrrole nitrogens.

and H_2TAP. This result is a natural consequence of the percent composition of the lowest empty $e_g(\pi^*)$ orbitals in ZnTAP and ZnPc which have a 21.8% N_9, 31.3% N_5 and 24% N_9, 24.7% N_5 composition, respectively. The best agreement with the experimental values is obtained either from the bonded model or from the bridged model XXII with a relatively short H_{20}–N_4 distance. Although these EH calculations are not able to unambiguously assign the best configuration, it must be remembered that Weiss *et al.* [3a] obtained a calculated Δ of 1870 cm^{-1} by assuming a bonded geometry. Our results indicate that small changes in ring geometry will lead to measurable changes in Δ. The 181 cm^{-1} increase in the $Q_x - Q_y$ splitting upon changing the solvent from pyridine to chlorobenzene [39, 40] can be interpreted on this basis.

Computer time for these EH calculations is normally reduced by assuming that the molecule of interest has two planes of symmetry. In all previously discussed calculations, this requirement has been met. If we consider a bonded configuration of H_2TAP or H_2Pc with the D_{2h} skeletal symmetry of Robertson [21], the resulting structure does not have two planes of symmetry. This structure is important, however, in order to test our previous assumption that in the bonded model the perturbation due to the central H atoms is much greater than that due to the distortion of the skeleton. Since calculations on such a structure of H_2Pc would be too costly, we considered the case of H_2TAP with C_{2h} molecular symmetry.

As can be seen from the results of such a calculation (Table 6 and Fig. 7), the properties of this configuration should be very similar to those of bonded H_2TAP with D_{4h} skeletal symmetry. This result confirms that indeed the main per-

turbation on the molecule is the bonding protons. From a study of the intrinsic polarization of the fluorescence of H_2TAP [41], it was concluded that the symmetry of the molecule was D_{2h}. Although the molecular symmetry of the configuration under consideration is formally C_{2h}, the symmetry of the π electron orbitals is essentially still D_{2h}. Consequently, the selection rules for such a configuration should be effectively equivalent to one that is formally D_{2h}.

The neutron diffraction study on H_2Pc indicates that the protons are not exactly on the line connecting the two nitrogen atoms, N_9–$N_{9'''}$ of Fig. 4. Physically, this corresponds to an increase in the amount of H-bonding with the bridged nitrogen atoms. Although the effect of placing H_{20} and $H_{20'}$ closer to N_{10} and $N_{10'}$ respectively (case 11) is slight, it does result in a smaller calculated value of Δ. The MO diagram for bonded H_2TAP with D_{2h} skeletal symmetry (case 10) closely resembles that of bonded H_2TAP with D_{4h} skeletal symmetry (case 1), even with respect to the $N_{p\sigma}$ orbitals. Although the above discussion is specifically about H_2TAP, similar results are expected for C_{2h} H_2Pc.

Other Work

A Mulliken population analysis [42] for various geometries of H_2P, H_2Pc, H_2TBP, and H_2TAP are reported elsewhere [17b]. The charge density of all atoms except the central hydrogens and the pyrrole nitrogens are fairly insensitive to changes in geometry. Generally, we find that the net charge of the pi electron SCMO–PPP calculations for H_2P [3] and H_2Pc [9] correlates with the net charge for all valence electrons in the EH model. Ref. [17b] also includes the following: additional calculations on various geometries of H_2Pc; a population analysis for the top filled and lowest empty orbitals of H_2P and H_2Pc; and a more complete discussion of some of our results.

Conclusions

We have discussed the splitting of the two Q bands in the free bases of four porphyrin related skeletons in terms of the energy gap between the vacant orbitals $b_{2g}(\pi^*)$, $b_{3g}(\pi^*)$ that are the degenerate $e_g(\pi^*)$ of the metal. We have been led to the following conclusions:

(1) The splitting is determined not only by the central H atoms but by distortions of the carbon-nitrogen skeleton. Changes in these distortions can account for the dependence of the $Q_x - Q_y$ split on environment.

(2) To obtain splittings of 700 cm^{-1} or more by a bridged structure, either there is incipient NH bond formation between central hydrogen atoms and bridge nitrogens or there is substantial D_{2h} distortion. Both effects may work cooperatively, but even so they cannot explain the large $Q_x - Q_y$ splitting observed in vapor of H_2Pc.

(3) Because of the sensitivity of $Q_x - Q_y$ splitting to environment in H_2Pc, the "isolated molecule" splitting suitable for the crystal may not correspond to either vapor or solution observations.

(4) $n-\pi^*$ transitions occur at lower energies in H_2TAP and H_2Pc than in H_2P or H_2TBP and may account for the great broadening of the Soret region of the former two compared to the latter.

(5) The only case where a bridged structure is likely is solution H_2Pc. Even here the calculations do not altogether rule out a bonded structure.

Acknowledgments. The research was supported in part by Public Health Services Research Grant GM-14292 from the Institute of General Medical Sciences. Professor E. R. Davidson let us use a new symmetrized extended Hückel program that he prepared for our C_{2h} calculation.

References

1. Paper I: Gouterman, M.: J. molecular Spectroscopy **6**, 138 (1961).
2a. Paper XV: Edwards, L., Gouterman, M.: J. molecular Spectroscopy **33**, 292 (1970).
b. Edwards, L.: Ph. D. Thesis, Committee on Chem. Phys., Harvard University, 1969.
3a. Paper III: Weiss, C., Kobayashi, H., Gouterman, M.: J. molecular Spectroscopy **16**, 415 (1965).
b. Paper XXIV: McHugh, A. J., Gouterman, M., Weiss, C.: Theoret. chim. Acta (Berl.) **24**, 346—370 (1972).
4. Sundbom, M.: Acta chem. Scand. **22**, 1317 (1968).
5a. Mathur, S. C.: J. chem. Physics **45**, 3470 (1966).
b. — McKannon, E. C.: Int. J. Quant. Chem. Symp. (No. 1), 247 (1967).
c. Klasino, L., Nowakowski, J.: J. chem. Physics **49**, 3326 (1968).
6. Chen, I.: J. molecular Spectroscopy **23**, 131 (1967).
7. Day, P., Williams, R. J. P.: J. chem. Physics **37**, 567 (1962).
8. Harrison, S. E.: J. chem. Physics **50**, 4739 (1969).
9. Sukigara, M., Nelson, R. C.: Molecular Physics **17**, 387 (1969).
10. Chen, I.: J. chem. Physics **51**, 3241 (1969).
11. Paper IV: Zerner, M., Gouterman, M.: Theoret. chim. Acta (Berl.) **4**, 44 (1966).
12. Paper V: — — Inorg. Chem. **5**, 1699 (1966).
13. Hamor, M. J., Hamor, T. A., Hoard, J. L.: J. Amer. chem. Soc. **86**, 1938 (1964).
14. Webb, L. E., Fleisher, E. B.: J. Amer. chem. Soc. **87**, 667 (1965).
15. Silvers, S., Tulinsky, A.: J. Amer. chem. Soc. **86**, 927 (1964).
16a. Chen, B.: Ph. D. Thesis, Department of Chemistry, Michigan State University, 1971.
b. — Tulinsky, A.: To be published.
17a. Schaffer, A. M., Gouterman, M.: Theoret. chim. Acta (Berl.) **18**, 1 (1970).
b. — Ph. D. Thesis, Department of Chemistry, University of Washington, 1972.
18. Antenson, J. E.: Ph. D. Thesis, Department of Chemistry, University of Pennsylvania, 1969.
19a. Paper XVI: Edwards, L., Gouterman, M., Dolphin, D. H.: J. molecular Spectroscopy **35**, 90 (1970).
b. Paper XVII: — Dolphin, D. H., Gouterman, M., Adler, A. D.: J. molecular Spectroscopy **38**, 16 (1971).
20. Anex, B. G., Umans, R. S.: J. Amer. chem. Soc. **86**, 5026 (1964).
21. Robertson, J. M.: J. chem. Soc. **1936**, 1195.
22. Fleischer, E. B.: Chem. Comm. **1970**, 105.
23. Berezin, B. D.: Russ. J. physic. Chem. **39**, 165 (1965).
24. Sharp, J. H., Landon, M.: J. physic. Chem. **72**, 3230 (1968).
25. Hoskins, B. F., Mason, S. A., White, J. C. B.: Chem. Comm. **1969**, 554.
26. Gurinovich, I. F.: Zh. Prikl. Spektrosk. **6**, 657 (1967).
27. Vincett, P. S., Voigt, E. M., Rieckoff, K. E.: J. chem. Physics **55**, 4131 (1971).
28. Schaffer, A. M.: Unpublished calculation.
29. Hochstrasser, R. M., Marzzacco, C.: J. chem. Physics **49**, 971 (1968).
30. Fielding, P. E., MacKay, A. G.: J. chem. Physics **38**, 2777 (1963).
31. — — Aust. J. Chem. **17**, 750 (1964).
32. Lyons, L. E., Walsh, J. R., White, J. W.: J. chem. Soc. **1960**, 167.

33. Lucia, E. A., Verderame, F. D.: J. chem. Physics **48**, 2674 (1968).
34. Vogt, L. H., Jr., Zalkin, A., Templeton, D. H.: Inorg. Chem. **6**, 1725 (1967).
35. Brown, C. J.: J. chem. Soc. (A), **1968**, 2488, 2494.
36. Robertson, J. M.: J. chem. Soc. **1939**, 1809.
37. Solov'ev, K. N., Shkirman, S. F., Kachura, T. F.: Bull. Acad. Sci. USSR, Phys. Ser. **27**, 763 (1963).
38. Woodward, I.: J. chem. Soc. **1940**, 601.
39. Stern, A., Pruckner, F.: Z. physik. Chem. (Leipzig) **178** A, 420 (1937).
40. Linstead, R. P., Whalley, M.: J. chem. Soc. **1952**, 4839.
41. Gurinovitch, G. P., Sevchenko, A. N., Solov'ev, K. N.: Optics and Spectroscopy **10**, 396 (1961).
42. Mulliken, R. S.: J. chem. Physics **23**, 1833, 1841 (1955).
43. Lucia, E. A., Marino, C. P., Verderame, F. D.: J. molecular Spectroscopy **26**, 133 (1968).
44. Barrett, P. A., Linstead, R. P., Rundall, F. G., Tuey, G. A. P.: J. chem. Soc. **1940**, 1079.

Dr. Arnold M. Schaffer
Department of Chemistry
University of Houston
Houston, Texas 77004, USA

Prof. Dr. Martin Gouterman
Department of Chemistry
University of Washington
Seattle, Washington 98105, USA